
**AFRL-OSR-VA-TR-2014-0059**

# PROTEINACEOUS LIGHT DIFFUSERS AND DYNAMIC 3D SKIN TEXTURE IN CEPHALOPODS

**ROGER HANLON**

**MARINE BIOLOGICAL LABORATORY**

**02/24/2014**
**Final Report**



**AIR FORCE RESEARCH LABORATORY**
**AF OFFICE OF SCIENTIFIC RESEARCH (AFOSR)/RSL**
**ARLINGTON, VIRGINIA 22203**
**AIR FORCE MATERIEL COMMAND**

# REPORT DOCUMENTATION PAGE

*Form Approved*
*OMB No. 0704-0188*



| **1. REPORT DATE** *(DD-MM-YYYY)* | **2. REPORT TYPE** | **3. DATES COVERED** *(From - To)* |
|---|---|---|
| 19/02/2014 | Final Report | |

**4. TITLE AND SUBTITLE**

Proteinaceous light diffusers and dynamic 3-D skin texture in cephalopods

**5a. CONTRACT NUMBER**
n/a

**5b. GRANT NUMBER**
FA9550-09-1-0346

**5c. PROGRAM ELEMENT NUMBER**
n/a

**6. AUTHOR(S)**
Hanlon, Roger T., Dr.

**5d. PROJECT NUMBER**
n/a

**5e. TASK NUMBER**
n/a

**5f. WORK UNIT NUMBER**
n/a

**7. PERFORMING ORGANIZATION NAME(S) AND ADDRESS(ES)**
Marine Biological Laboratory
7 MBL Street
Woods Hole MA 02543-1015

**8. PERFORMING ORGANIZATION REPORT NUMBER**

**9. SPONSORING / MONITORING AGENCY NAME(S) AND ADDRESS(ES)**
USAF, AFRL
AF Office of Scientific Research
875 N. Randolph Street, Room 3112
Arlington VA 22203

**10. SPONSOR/MONITOR'S ACRONYM(S)**

**11. SPONSOR/MONITOR'S REPORT NUMBER(S)**

**12. DISTRIBUTION / AVAILABILITY STATEMENT**

**13. SUPPLEMENTARY NOTES**

**14. ABSTRACT**

This project discovered fundamental and novel mechanisms of structural coloration in cephalopods as well as the biomechanics of dynamic skin papillae that produce morphing soft skin. Two mechanisms of producing whiteness in flexible skin were revealed. First, spherical proteinaceous leucosomes produce uniform and highly efficient whiteness in all directions and from all viewing angles. Second, proteinaceous platelets in specific arrangements can also produce diffuse whiteness, but not with the efficiency of spherical leucosomes. Skin papillae that dynamically produce morphing 3D skin were also characterized biomechanically via gross and fine morphology; they are basically constructed as a muscular hydrostat (similar to a human tongue, elephant trunk, or octopus arm). For each research project, sufficient modeling of the structures and spectrometry was accomplished and published to enable initial stages of transfer to materials science. An additional project involved dynamic structural coloration of iridophores; the neurophysiological control of iridescence was discovered to involve aspects of peripheral control (as opposed to solely brain control). In addition to biological achievements, this grant developed new methodology for high-resolution imaging of coloration elements in biological tissue.

**15. SUBJECT TERMS**

| **16. SECURITY CLASSIFICATION OF:** | | | **17. LIMITATION OF ABSTRACT** | **18. NUMBER OF PAGES** | **19a. NAME OF RESPONSIBLE PERSON** |
|---|---|---|---|---|---|
| **a. REPORT** | **b. ABSTRACT** | **c. THIS PAGE** | | | **19b. TELEPHONE NUMBER** *(include area code)* |

**Standard Form 298 (Rev. 8-98)**
**Prescribed by ANSI Std. Z39.18**

To: technicalreports@afosr.af.mil
Subject: Final Performance Report to Dr. Hugh De Long

**Proteinaceous light diffusers and dynamic 3-D skin texture in cephalopods**

Grant #: FA9550-09-0346
Reporting period: 1 May 2009 – 3 November 2013

PI: Roger T. Hanlon, Marine Biological Laboratory, Woods Hole, MA 02543

## Executive Summary

This project discovered fundamental and novel mechanisms of structural coloration in cephalopods as well as the biomechanics of dynamic skin papillae that produce morphing soft skin. Two mechanisms of producing whiteness in flexible skin were revealed. First, spherical proteinaceous leucosomes produce uniform and highly efficient whiteness in all directions and from all viewing angles. Second, proteinaceous platelets in specific arrangements can also produce diffuse whiteness, but not with the efficiency of spherical leucosomes. Skin papillae that dynamically produce morphing 3D skin were also characterized biomechanically via gross and fine morphology; they are basically constructed as a muscular hydrostat (similar to a human tongue, elephant trunk, or octopus arm). For each research project, sufficient modeling of the structures and spectrometry was accomplished and published to enable initial stages of transfer to materials science. An additional project involved dynamic structural coloration of iridophores; the neurophysiological control of iridescence was discovered to involve aspects of peripheral control (as opposed to solely brain control). In addition to biological achievements, this grant developed new methodology for high-resolution imaging of coloration elements in biological tissue.

## Archival Publications (published) during the reporting period:

Deravi, L.F., Magyar, A.P., Sheehy, S.P., Bell, G.R.R., Mathger, L.M., Senft, S.L., Wardill, T.J., Lane, W.S., Kuzirian, A.M., Hanlon, R.T., Hu, E.L. and Parker, K.K. 2014. In press. **The structure-function relationship of a natural nanoscale photonic device in cuttlefish chromatophores**. J. Royal Society Interface

Gonzalez-Bellido PT, Wardill TJ, Ulmer KM, Buresch KC, Hanlon RT. 2014 in press. **Expression of squid iridescence depends on environmental luminance and peripheral ganglion control.** Journal of Experimental Biology

Allen JJ, Bell GRR, Kuzirian AM, Velankar SS, Hanlon RT. 2014 in press. **Comparative morphology of changeable skin papillae in octopus and cuttlefish.** Journal of Morphology.

Mäthger LM, Senft SL, Gao M, Karaveli S, Bell GRR, Zia R, Kuzirian AM, Dennis PB, Crookes-Goodson WJ, Naik RR, Kattawar GW, Hanlon RT. 2013. **Bright White**

**Scattering from Protein Spheres in Color Changing, Flexible Cuttlefish Skin**. Advanced Functional Materials 23(32):3980-3989.

Kreit E, Mäthger LM, Hanlon RT, Dennis PB, Naik RR, Forsythe E, Heikenfeld J. 2013. **Biological versus electronic adaptive coloration: how can one inform the other?** J R Soc, Interface 10(78): article 20120601.

Allen JJ, Bell GRR, Kuzirian AM, Hanlon RT. 2013. **Cuttlefish skin papilla morphology suggests a muscular hydrostat function for rapid changeability**. Journal of Morphology 274(6): 645-656.

Bell GRR, Kuzirian AM, Senft SL, Mathger LM, Wardill TJ, Hanlon RT. 2013. **Chromatophore radial muscle fibers anchor in flexible squid skin**. Invertebrate Biology 132(2):120-132.

Gonzalez-Bellido PT, Wardill TJ. 2012. **Labeling and Confocal Imaging of Neurons in Thick Invertebrate Tissue Samples**. Cold Spring Harbor Protocols 2012(9):pdb.prot069625.

Mäthger LM, Bell GRR, Kuzirian AM, Allen JJ, Hanlon RT. 2012. **How does the blue-ringed octopus (*Hapalochlaena lunulata*) flash its blue rings?** J Exp Biol 215(21):3752-3757.

Wardill TJ, Gonzalez-Bellido PT, Crook RJ, Hanlon RT. 2012. **Neural control of tuneable skin iridescence in squid**. Proceedings of the Royal Society B 279(1745):4243-4252.

Hanlon RT, Chiao CC, Mäthger LM, Buresch KC, Barbosa A, Allen JJ, Siemann L, Chubb C. 2011. **Rapid adaptive camouflage in cephalopods**. Pgs. 145-163. In: Stevens M, Merilaita S, editors. Animal camouflage: mechanisms and functions. Cambridge, U.K.: Cambridge University Press.

Submitted Publications:

Bell GRR, Mäthger LM, Gao M, Senft SL, Kuzirian AM, Kattawar GW, Hanlon RT. Submitted. **Diffuse white structural coloration from multilayer reflectors in a squid.** Advanced Materials.

Kripke, E., Senft, S., Mozzherin, D. and Hanlon, R.T. Submitted. **Visualizing biological complexity in cephalopod skin: a synergy of art and science technologies**. Leonardo

PhD dissertation:

Allen, J.J. **3D skin: Functional morphology of cuttlefish and octopus papillae, filefish dermal flaps, and their use in camouflage**
Brown/MBL Joint PhD Program in Neuroscience, Brown University, Providence, R.I.

Non-refereed papers:
Mathger, LM & Hanlon, RT. 2014. Dynamic displays in nature. Information Display 1/14: 2-6.

Changes in research objectives: Only one minor change occurred. In 2012, the responsibility for modeling leucophore reflection was shifted from Brown University (Prof. Rashid Zia) to Texas A&M (Prof. George Kattawar). Professor Zia continued to refine their novel new microscope for this effort.

Change in AFOSR program manager: None
Extensions granted or milestones slipped: None
New discoveries, inventions, or patents: N/A

## Background

Adaptive camouflage and signaling are key elements of natural selection and are of obvious importance to military and intelligence operations. Natural selection has honed thousands of such systems, yet it is agreed that rapid adaptive coloration is best developed in the cephalopods, a thriving group of marine mollusks that include squid, octopus, and cuttlefish. Our focus is on ultrastructure, optical output from the skin, and modeling that may yield bio-inspired approaches to materials development.

Cephalopod skin provides a biological template for solving two major issues:

1) Angle-independent white light reflection, which is accomplished by leucophore cells containing randomly distributed proteinaceous spheres;

2) Morphing papillae that are capable of altering the 3D texture of the skin for camouflage in complex 3-D habitats. Both of these systems have implications for materials design; the leucophores could serve as the white base-layer in reflected light systems while the papillae provide biological inspiration for materials that change shape and texture.

## Objectives

Leucophores

Aim 1: Spectrometry. Quantitatively characterize leucophore reflectance properties (spectral reflectance UV-IR, polarization, diffusing properties) in cephalopod and fish species.

Aim 2: Ultrastructural analysis. Determine the cellular architecture that enables scattering of light using light, electron and confocal microscopy.

Aim 3: Modeling & Measurement – From Leucosome Scatterers to Leucophore Diffusers

Aim 4: Protein chemistry. Collaborate with AFRL (R.Naik) to characterize the cephalopod leucophore protein(s).

Morphing papillae

Aim 1: Ultrastructural analysis. Determine the muscular arrangement that provides the morphing capability of cephalopod papillae (e.g., muscular hydrostat, buckling mechanism, etc.).

Aim 2: Neurophysiological control. Use electrophysiology and neural tracing methods to determine CNS control of papillae.

Aim 3: Videography of dynamic conformational change.

## New Findings

### 1. Diffuse white reflection

Leucophores are angle-independent structural reflector cells composed of many small spherical proteinaceous scatterers known as leucosomes. Collectively these cells diffuse white light equally well in all directions; i.e. they appear to be nearly "perfect" diffusers (Figure 1 A-C). A main focus of this grant was to determine the optical, physical, biochemical properties of the leucophore system.

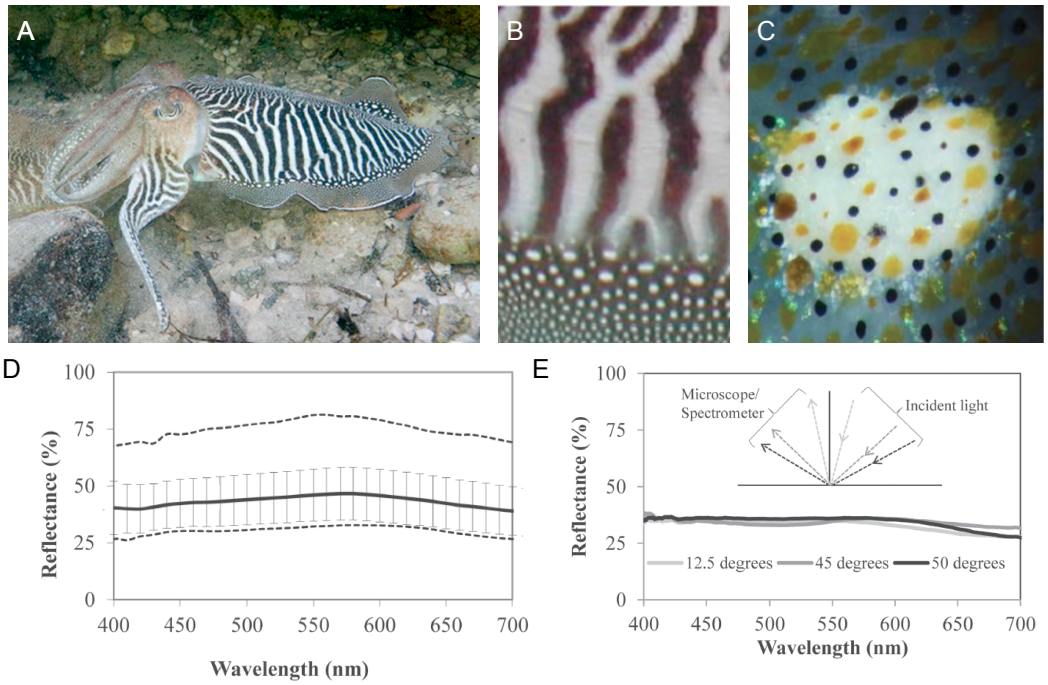


**Figure 1.** Fin spot spectroscopy **A.** Adult cuttlefish *Sepia officinalis* exhibiting a high contrast pattern. **B.** Close up of the bold zebra-stripe pattern and the white fin spots located at the bottom of the image. **C.** Micrograph of a single white fin spot underneath pigmented chromatophores. **D.** Broadband reflectance of whole fin spots, dashed lines: maximum (75%) and minimum (30%) reflectance range, solid line: average reflectance (45%), n=50. **E.** Fin spot reflectance measured at varying illumination/viewing angles; fin spots yield angle independent reflection.

Leucophores occur in many regions of the cuttlefish skin; however, by far the brightest white is observed in the fin spots and these are enriched with leucophores. These white markings reflect broadly across the ultraviolet, visible, and near infrared

(300-1000 nm). Spectral reflectance of fin spots, measured with an Ocean Optics Spectrometer, ranged from ~30% to ~75%, averaging ~45% (Figure 1 D). Fin spots were also observed to reflect broadband light independent of illumination/viewing angle (Figure 1 E).

Leucophores have no attached nerves or muscle fibers and appear to be physiologically passive; that is, their biological energy requirements for scattering are low or nil. We tested the following drugs that are known to play a role in the activation of other skin structures in cephalopods and fish (chromatophores and/or iridophores): serotonin (5-HT; relaxes cephalopod chromatophore muscles), L-glutamic acid (contracts cephalopod chromatophore muscles), acetylcholine (ACh; activates cephalopod iridophores), potassium chloride (KCl; depolarizes cell membranes), norepinephrine (activates fish chromatophores). We found that none of these compounds affected the reflectance of cuttlefish leucophores.

A 3-D electron microscopy data set (1 mm x 1 mm x 0.75 mm) of a cuttlefish fin spot was acquired using a Gatan 3View Serial Block Face Imaging (SBFI) system. Within the bounds of this high-resolution data set we identified one complete leucophore that was composed solely of proteinaceous spheres. Using analysis software developed by Steve Senft (MBL), we extracted the x, y, and z coordinates of the spherical leucosomes as well as their radii (Figure 2 A).

To model light reflection from the leucophore extracted from the Gatan data we also needed to measure the refractive index of the leucosomes. Leucophores were isolated from protease-digested fin spots, placed in deionized water and coverslipped with a 150 µm spacer. The cells were intentionally ruptured via changes in osmolarity, and the spacer allowed the particles to move via Brownian motion, which permitted an averaging of the background that improved the accuracy of the measurement. Rashid Zia and Sinan Karaveli from Brown University measured the refractive index for individually tracked leucosomes using in-line digital holographic microscopy. The average refractive index was $1.51 \pm 0.02$ (Figure 2 B).

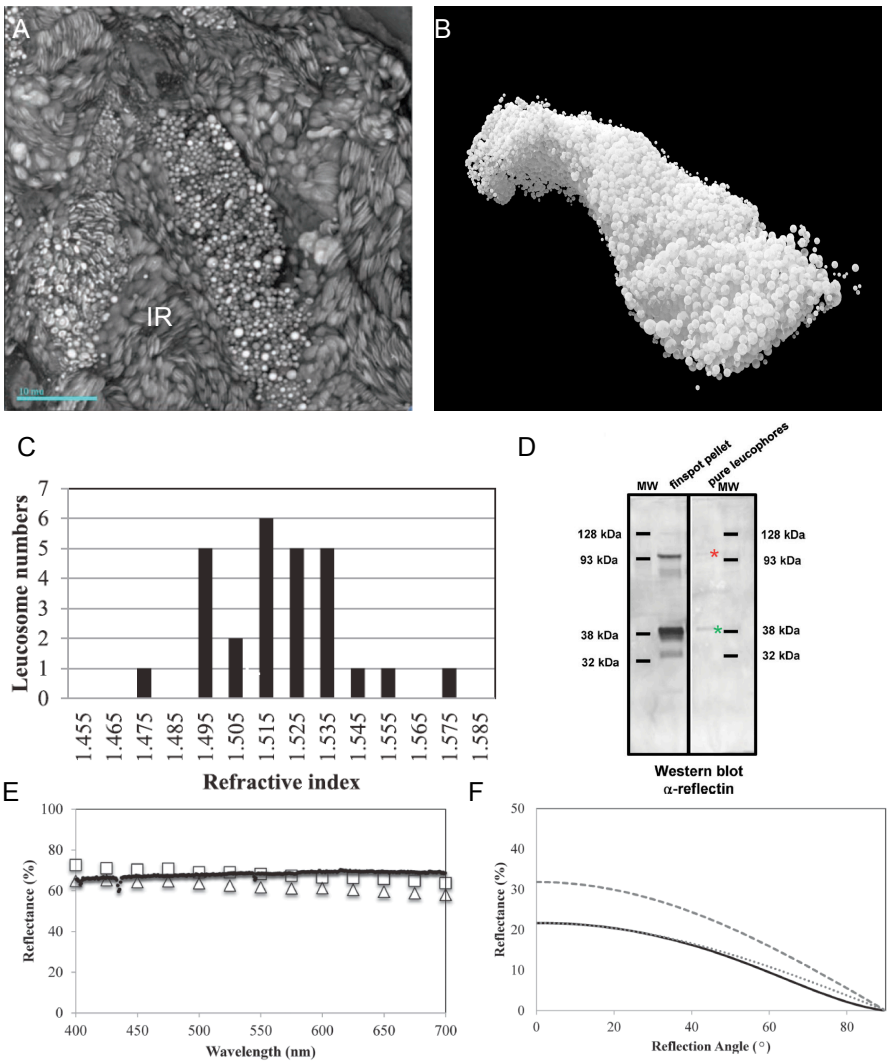


**Figure 2.** Leucophore physical and chemical characteristics. **A.** Volume rendering of a subset of the 3D electron microscopy data, showing packing of leucosomes within a single leucophore (L). Surrounding platelets are from adjacent iridophores (IR). **B.** Rendering (using Blender software) of simulated leucosomes using radii and locations derived from a single leucophore. **C.** Measured refractive index for 27 individual leucosomes. Average refractive index: 1.51 ± 0.02. Histogram show refractive index distribution. **D.** Purified leucophores were resolved in toto with SDS-PAGE followed by Western blotting and probing with the reflectin antibody (right panel). Green asterisk shows a 38 kDa reflectin positive band, red asterisk indicates the location of an additional, 93 kDa reflectin-positive band (weaker in comparison with others). A lane containing the insoluble fin spot fraction was added for direct comparison (left panel). **E.** Simulations show that the fin spot system approximates a Lambertian surface. Dots: measured reflectance (from 400-700 nm) from cuttlefish fin spot can be as high as ~70%, reflecting equally well across the visible spectrum. Triangles: modeled flux reflectance spectrum averaged over all reflection angles and for 0° incidence. Squares: the normalized reflectance spectrum obtained by normalizing the modeled reflectance to a perfect Lambertian reflector. **F.** Modeled angular reflectance averaged over the visible spectrum. The modeled angular distribution (solid line) is close to a cosine function (represented by the dotted line) typical of a Lambertian surface. The dashed line is the angular distribution ($\cos\theta/\pi$) of a perfect Lambertian surface, having 100% total reflectance integrated over $2\pi$ solid angle.

We were interested in relating the biophysical properties of leucosomes with the bulk optical properties of the tissue from which they were obtained. The Fourier-based optical measurements that provided refractive index simultaneously determined a range of sizes for the unfixed leucosomes of 600 to 800 nm. Our 3D Gatan EM data was sampled isotropically at 50 nm, readily resolving objects of this size, and analysis of the spheres identified in that aldehyde-fixed and epon-embedded material yielded an average diameter of 750 nm. This correspondence suggests that the leucosomes were little changed by fixation; in contrast, tissue prepared for electron microscopy tends to shrink, overall, on the order of up to 25%.

These morphometric statistical values were used in tandem with the experimentally determined refractive index values to simulate light scattering off a tissue containing leucophore cells. The leucosomes number density was determined from analysis of the 3D Gatan data. A Monte Carlo method was used to calculate the reflectance of this system at a variety of wavelengths and angles. At each angle the results were normalized to that of a perfect Lambertian reflector. The system thickness of the model was adjusted so that the overall computed reflectance (68%) matched the reflectance measured from the fin spots. Comparison of tissue with computed reflectivity shows close correspondence across the visible spectrum: both reflectivities are nearly independent of wavelength, i.e. white. Both the fin spots and the computed systems are brighter in proportion to thickness.

Leucophore protein composition was determined in collaboration with Wendy Crooks-Goodson, Patrick Denis and Rajesh Naik from AFRL. Proteomic analysis was performed on material extracted from dissected, homogenized fin spots. Post homogenization, the extracts were centrifuged, the pellet was run using SDS-PAGE and the individual bands were analyzed using MALDI-TOF and Tandem mass spectrometry for sequence determination of select peptides. Analysis of each protein species indicated homology to several squid reflectin isoforms. No non-reflectin-like proteins were identified in the finspot samples.

Fin spots contain both leucophores (spheres) and iridophores (platelets), thus we were interested in isolating pure leucophores for further analysis. Fin spots were dissociated using enzymatic digestion (collagenase), and individual leucophores were collected using laser capture micro-dissection. The small, but highly enriched leucophore sample was run on a SDS-PAGE gel and directly analyzed by Western Blotting using the anti-reflectin antibody. A cross-reactive band was observed at the predicted molecular weight of the squid reflectin monomer (40 kDa), as well as at the higher 110 kDa band (possible multimer) (Figure 2 C). This indicates that cuttlefish proteins related to the squid reflectins are present in the leucophores and may play a role in the formation and function of light scattering in leucosomes.

In 2013, we published a comprehensive manuscript in Advanced Functional Materials (Mathger et al., 2013) on leucophore white light scattering. In this manuscript, we describe the optical properties of the diffuse white and unpolarized scattering structures (leucophores) in cuttlefish skin. We report data on spectrometry (spectral measurements of whole leucophore structures, covering UV, visible and IR wavelengths, polarization and angle dependent properties), ultrastructure (collaboration with Gatan Inc., Pleasanton, CA), to acquire images using their 3View serial block-face scanning electron microscopy system, holographic microscopy to determine refractive index

(collaboration with Brown University), mathematical simulations, showing that the leucophore system is a random scattering photonic system (collaboration with TAMU) and protein analysis (collaboration with AFRL).

In summary, with help from our collaborators, we have established that the white reflectivity of the cuttlefish fin spot can be matched through Mie scattering by a collection of variously sized spherical sub-cellular particles averaging 700 nm in diameter, containing the protein reflectin. In contrast to conventional thin film diffusers that rely upon high-index contrast (e.g., using titania nanoparticles, RI > 2.5), leucophores appear to provide both high reflectivity and near-Lambertian scattering with a low-index (ca. 1.5) contrast system.

## 2. Morphing papillae.

Our work on the functional morphology of simple, conical Small dorsal papillae from cuttlefish (*Sepia officinalis*) skin was published in 2013 in the Journal of Morphology. Briefly, these papillae were found to consist of dermal erector muscles oriented in concentric rings or extending horizontally from one edge of a papilla to another. Contraction of the concentric dermal erector muscles lift the papilla away from the surface of the animal while contraction of the horizontal dermal erector muscles pull the edges of the papilla toward its core and determine its shape. Because the same muscles that are responsible for movement also provide structural support in the absence of rigid elements, the Small dorsal papillae *function as muscular hydrostats*.

We have built on this research by investigating the space between muscle cells in muscular core of these papillae. Staining with colloidal iron and Van Gieson's stain revealed glycosylated extracellular matrix in the core of each papilla, surrounding the dermal erector muscles. Putatively this extracellular matrix contributes to papilla structural support, and possibly functions as a hydrogel (Figure 3 A).

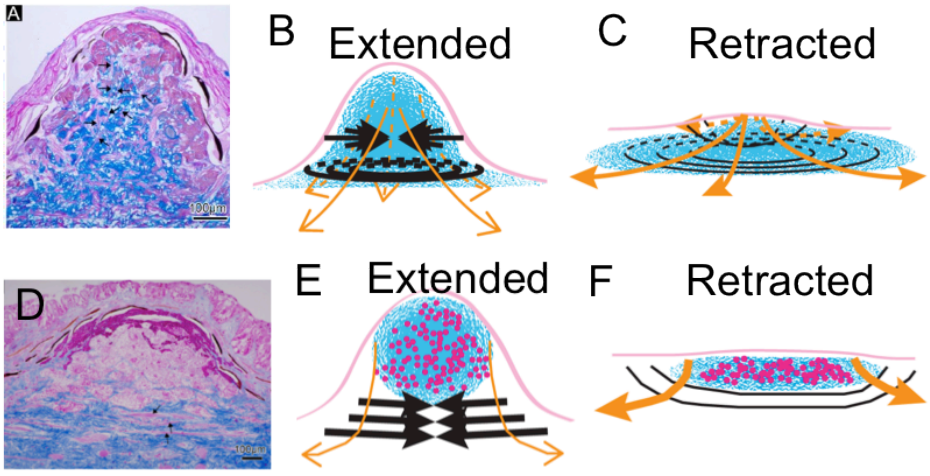


**Figure 3.** Papilla functional mechanisms (muscular hydrostat v buckling). **A.** *Sepia officinalis* Small dorsal papilla cut in cross section and stained with colloidal iron and Van Gieson's stain. Blue, connective tissue containing a polysaccharide element; pink, collagen; salmon, muscle; pink-orange, reflectors; dark brown, chromatophores. Black arrows indicate a radiating retractor muscle. **B-C.** Muscular hydrostatic extension (left ) and retraction (right). Retractor muscles (orange) radiate from the apex of the papilla to oppose concentric circular and horizontal dermal erector muscles (black). The polysaccharide containing extracellular matrix is represented in blue. **D.** *Sepia apama* face wrinkle cut in cross section and stained

with Mallory's Trichrome. Pink on perimeter, epidermis; dark pink, reflectors (leucophores and iridophores), blue, collagen; brown and yellow, chromatophores; medium pink, muscles. Black arrows indicate buckling muscles. **E.** Buckling muscles (black) in *S. apama* contract to lift reflectors away from the surface of the face and arms. **F.** Retractor muscle (orange) activation flattens the face wrinkle. Blue, glycosylated extracellular matrix; pink, leucophores.

Our newly published data support an active retraction mechanism for these papillae. We have identified muscles that run from the periphery to the apex of the papilla. These muscles are typically located along the perimeter of the papilla, between the muscular core and the overlying reflectors. This location and orientation suggests that contraction of these retractor muscles opposes the dermal erector muscles, flattening the papilla (Figure 3 A-C).

Comparative functional morphology (Allen et al. in press 2014) has been studied in papillae of different shapes and sizes for several cuttlefish and octopus species: (i) face ridges from Sepia apama, (ii) Small and Ventral eye papillae from *Octopus vulgaris*, (iii) Dorsal eye papillae from *Macrotritopus defilippi*, (iv) mantle, arm ridge and Dorsal eye papillae from *Octopus bimaculoides*. Briefly, the *S. apama* face ridges function via a buckling mechanism where dermal erector muscles underlie a mass of reflectors (Figure 3 D). Contraction of these muscles lifts the reflectors away from the surface of the face and arms, creating the ridge (Figure 3 E-F). In this case the reflectors – not the muscles – provide the structural support. All other papillae studied showed variations on the muscular hydrostat theme: all had dermal erector muscles, a muscular core, and separate retractor muscles.

We have used an electrophysiology preparation developed within this laboratory to show that nerves in the skin if activated electrically will result in the expression of papillae. Papilla expression achieved through neural stimulation was relatively slow (6 seconds; Figure 4). However, since there are antagonistic muscle groups responsible for retracting papillae, this may have been due to non-selective activation of both sets of muscles resulting from stimulating the entire nerve bundle. We were only partially successful in activating axons that innervate the individual muscle groups in a coordinated fashion.

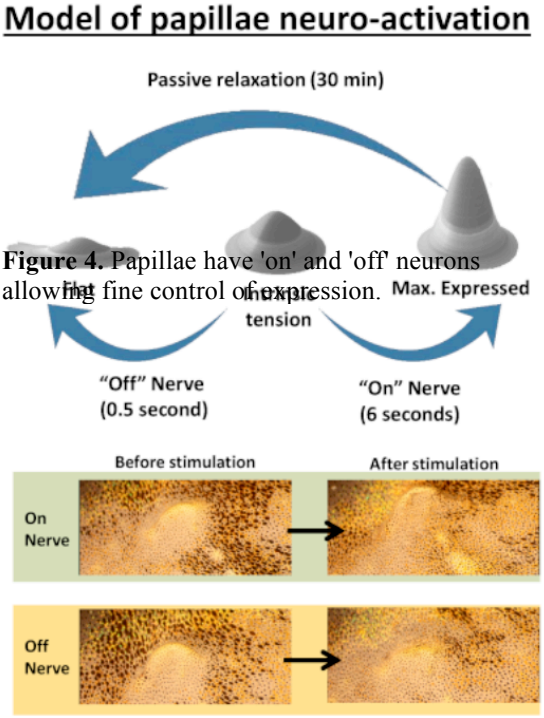


**Figure 4.** Papillae have 'on' and 'off' neurons allowing fine control of expression.

To better understand this complex system we searched for the origin of neurons involved in controlling papillae shape. In particular, we investigated whether the papillae neurons are located in the peripheral neural center (the stellate ganglion) or whether they originate directly from the brain, as do chromatophore neurons. This effort may allow for manipulation of specific muscle types.

Papillae, like other molluscan systems, may contain "catch" muscles: muscles having the ability to maintain contractive force during prolonged periods with minimal energy consumption. Denervating (cutting) the pallial nerve, which contains neurons that travel to the mantle from the brain, on one side of the animal, resulted in a complete lack of chromatophore and fin muscle control ipsilateral to the cut (Figure 5). However, the papillae on the denervated side were "stuck" in the expressed position even when the animal retracted the papillae on the control (uncut) side. The results suggest that the papillae remained expressed because some or all of its muscles had entered a "catch" state prior to the pallial nerve cut. Known catch muscles are smooth, not striated. It is also known that catch muscles in other molluscan species use either acetylcholine or the neuropeptide, FMRFamide as neurotransmitters.

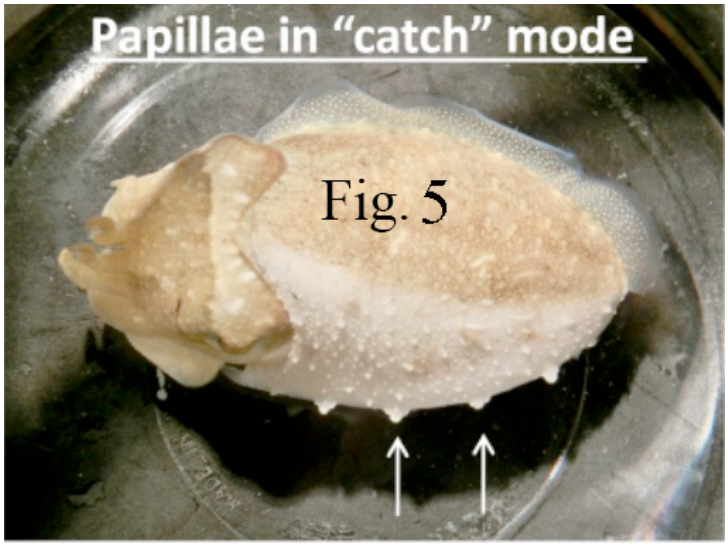


To investigate possible neurotransmitters responsible for papillae expression, we injected skin of freshly killed cuttlefish (*Sepia officinalis*) with FMRFamide, acetylcholine (ACh), glutamate and seawater (control). We found that FMRFamide and glutamate produced "buckling" or "bunching" of the skin, and the contractions produced by FMRFamide were long lasting. This contraction effect was not observed with ACh or seawater. However, ACh injection did result in papillae "caps" being expression. Thus at present, our working hypothesis is that ACh controls the upper, (distal cap) of the papillary shape, while FMRFamide and glutamate control the deeper, larger muscle groups, that are responsible for actually erecting the main body of the papillae. It is possible that both glutamate and FMRFamide are used in concert to provide either short, or long term papillae expression. Presently, we are combining electrophysiological papillae activation together with neurotransmitter blockers to elucidate whether specific papillae shape changes occur when certain neurotransmitters are blocked.

Through the imaging protocol developed last year, we can now provide images of the dorsal skin musculature that may be responsible for skin buckling and papillae expression. Initial images support the speculation these are smooth muscles and thus function as "catch" muscles.

With the lab of Sachin Velankar, UPitt, we conducted mechanical measurements of cuttlefish skin tissue (March 2012) with Dr. Derek Breid, a postdoctoral researcher. It was determined that the measurements were unreliable on cephalopod skin due to (i) unstimulated natural muscle movement, even many hours post-mortem, and (ii) muscle complexity, which made it difficult to separate the effects of the different layers. To provide a non-invasive measurement of the skin folding capability and pattern, Sachin's group developed new software to track the skin as it moves.

We have provided them videos of cephalopod skin contracting under electrical stimulation and neurotransmitter injections. The results showed that skin compresses (or strains) by 30% under experimental conditions. We are currently using this technique to detect in which direction the strains are largest, to quantify which neurotransmitters cause the strongest contraction and to elucidate if the folding pattern produced is related to the orientation of the muscles observed in the deeper layer of the dorsal skin.

## 3. Diffuse white light reflection from multilayer reflectors

We investigated diffuse white scattering from the Pyjama squid (Sepioloidea lineolata) (Figure 6 B-C). Unlike the Mie scattering structures found in cuttlefish leucophores, white light reflection in the Pyjama squid is achieved solely with iridophores (multilayer reflectors). Spectrally, the stripes reflect from approximately 300 nm to 950 nm, and average ~25% reflectance (Figure 6 C). When viewed close-up (e.g., 225x magnification), iridophores locally reflect narrow wavebands of light, but collectively these cells give the appearance of white light when viewed at a distance (Figure 6 D).

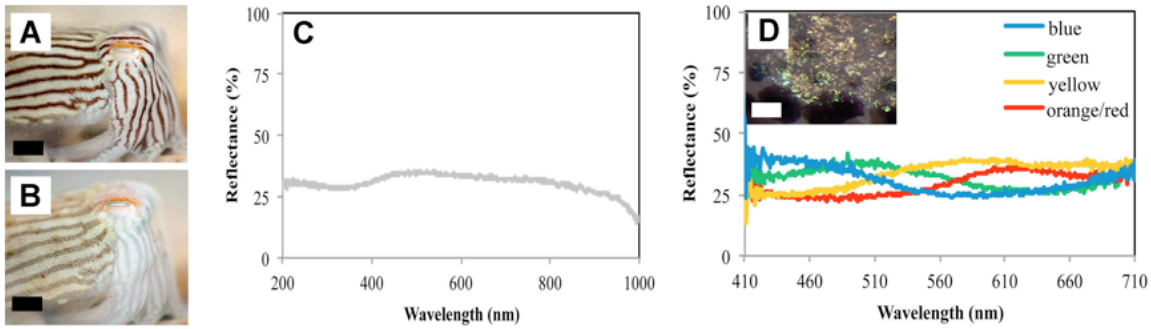


**Figure 6.** Optical/histologic properties of *S. lineolata* white stripe. **A.** High-contrast pattern; underlying iridophores and superficial brown chromatophores produce alternating white and dark stripes; scale: 4 mm. **B.** Low-contrast pattern, chromatophores retracted; scale: 4 mm. **C.** Broadband reflectance of white stripe (~40% from 200 nm-1000 nm). **D.** Variations in spectral reflectance (400nm – 700nm) observed at 225x. Inset: high magnification of white stripe; scale: 125 µm.

Morphometric analyses of transmission electron micrographs were conducted to extract plate orientation, plate thickness and inter-plate spacing values (Figure 7). The morphometric statistics were incorporated into the two-stream radiative transfer theory model (in collaboration with TAMU) to simulate white light diffusion for multiple viewing angles as well as the polarization of the system. Additionally, binarized TEM iridophore micrographs were inserted into a Finite Difference Time Domain (FDTD) model to simulate light reflection (Figure 8 A-C). This method preserves the spatial arrangement of the reflectors in cross-section. In both model systems the predicted light reflection closely matched the values measured directly from the tissue using spectroscopy. Iridophore reflection in other animals typically is highly angle dependent; however, the pyjama squid iridophore stripes reflect diffuse white light at angles from normal to approximately 35 degrees. At greater angles of incidence, the reflectance increases (Figure 8 D). The pyjama squid system is also weakly polarized (<20%) and is likely caused by the large distribution of iridophore plate angles (Figure 8 E).

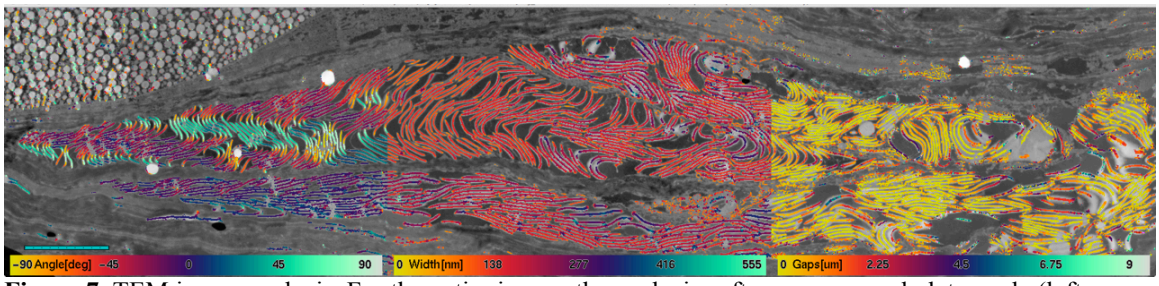


**Figure 7.** TEM image analysis. For the entire image, the analysis software measured plate angle (left panel), plate thickness (center panel), and inter-plate spacing (right panel). In the left panel, the colors indicate the range in plate orientation angles (0° = parallel to the skin surface). The center panel colors indicate the range in plate thickness (nm). The colors in the right panel indicate the maximum distance to the two nearest neighboring plates (inter-plate spacing; µm). This emphasizes the location of the stack edges. Scale: 5 µm.

The pyjama squid system is a superb example of an angle dependent, biological dielectric mirror system that reflects broadband light in an angle indendent (diffuse) manner. While this system is very interesting from a biological perspective, it also has implications for the materials community. In *Loliginid* squids, the reflector protein (reflectin) has been shown to be spectrally tunable by modulating plate thickness and interplate spacing; it is possible that a similar mechanism exists in the pyjama squid. In addition to spectral tuning it is possible that the animal could modulate the diffuse or specular nature of the reflected light by adjusting plate orientation.

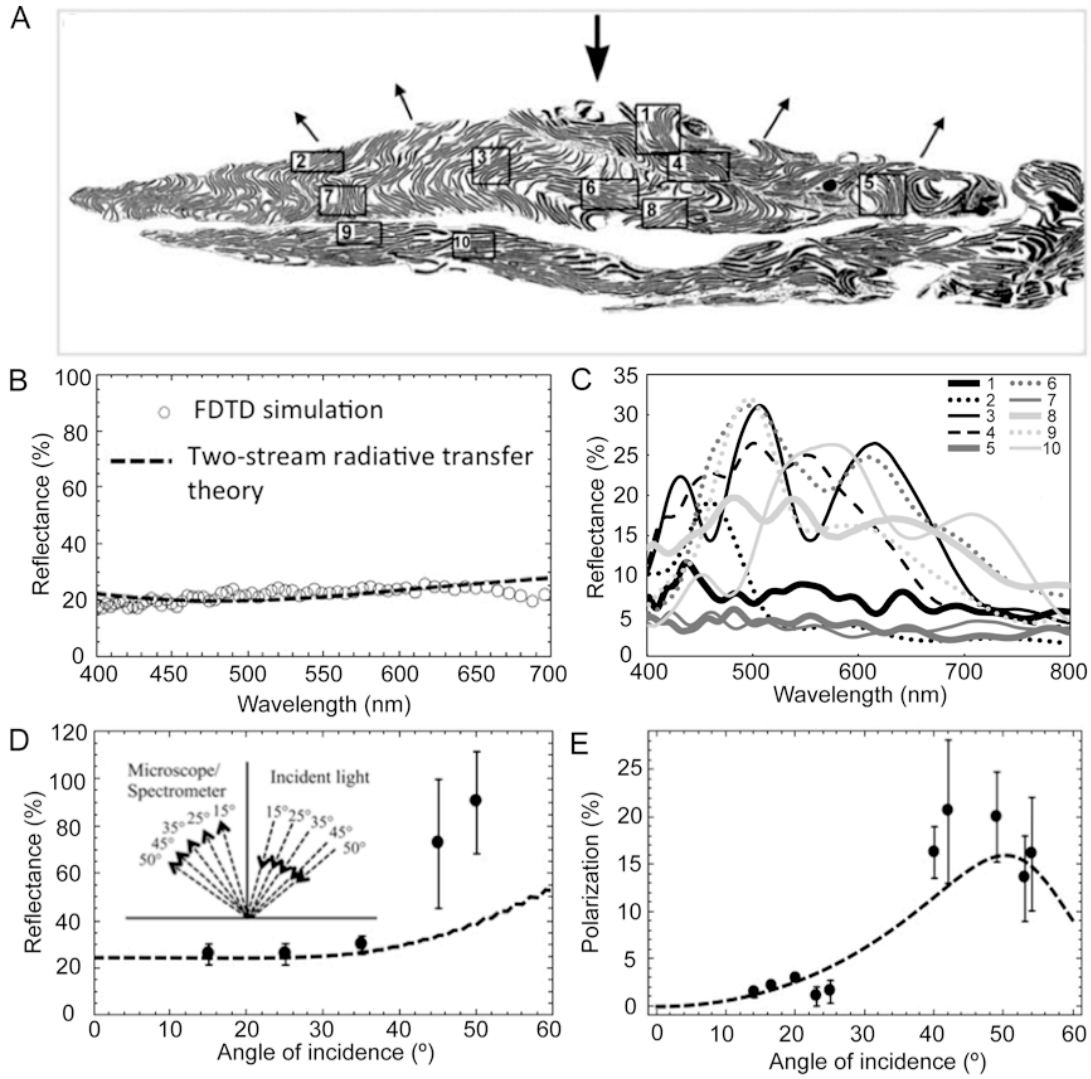


**Figure 8.** Measured and simulated optical properties. **A.** Binarized version of TEM panorama used in FDTD simulation; iridosome (black) refractive index=1.59[37]; inter-plate (white) refractive index=1.33. Outlined area indicates computational domain; large arrow indicates incident light direction, smaller arrows indicate reflected light. Sub-regions, boxes 1-10, were selected to model reflectance spectra from individual Bragg stacks. **B.** Predicted reflectance spectra for non-polarized light at normal incidence from FDTD simulation and two-stream radiative transfer theory. **C.** Predicted reflectance spectra for 10 sub-regions found in (A) using FDTD modeling. Low reflectance values are likely due to incoherent orientation of plates. **D.** At increasingly oblique viewing/incident angles, reflected light increases. Plot shows averages and s.e. (n=10). Inset shows set-up angles for measured data obtained using goniometer. Measurement direction was vertical, given by microscope position. Two-stream radiative transfer theory predicts that reflectance increases with incident angle (dashed line). **E.** Polarization measurements. At angles up to ~25°, polarization is low (~1-2%). At angles around Brewster's angle (50°), polarization increases to its maximum value but remains partial (~13-20%). Plot shows averages and s.e. (n=3). Two-stream radiative transfer theory corroborates the increase in polarization near Brewster's angle.

## 4. Determining neural control of squid iridophores containing active reflectors.

Our investigations of skin leucophores and iridophores led us to an additional finding. To determine the neural basis of iridophore control, we developed an isolated fin preparation that allows electrical stimulation and monitoring of neurons controlling the squid fin skin (*D. pealeii*). Using this preparation, we stimulated and measured iridophore responses for changes in spectral reflectance and brightness (Wardill et al. 2012). We also developed a whole mount preparation of cephalopod skin that allowed tracing of neurons from the main fin nerve to their respective skin element targets (Gonzalez-Bellido & Wardill 2012). Using both of these techniques, we demonstrated that iridophores are directly controlled by neurons, and that their spectral change has a faster response than their brightness change when neurally stimulated. Taking this neurobiology approach further, we developed a partial nerve denervation procedure that allowed us to determine that iridophores are controlled using a completely independent neural circuit that travels a new pathway not used by chromatophore motorneurons. Iridophore motorneuron cell bodies were identified to be located in the stellate ganglion (not the brain as found for chromatophore motorneurons), along with several motorneurons that control fin muscle movement. By testing squid in various light conditions, with chromatophore control compromised by targeted denervation, we also demonstrated that skin iridescence brightness is altered according to the ambient light level in which the squid is living (Gonzalez-Bellido et al. 2014 in press). Future investigations will determine if parts of the squid iridophore splotches are also neurally controlled diffusers based on some preliminary observations.

**Invited seminars: (**examples from 3x this many)
Rockefeller Univ; Natick Soldier Center US Army; East Coast Nerve Net Annual Meeting (plenary); International Conference of Computational Photography (plenary); Molluscan Neurobiology in Genomics Era (plenary); Visualizing Science course at MBL; Boston Fullbright Fellows; MIT Science Writers; UMass Lowell; Center for Vision Research, Brown University; Pan American Society for Pigment Research & Melanoma Annual Meeting (plenary); DSRC, DARPA; Brandeis University; Society for Integrative & Comparative Biology.